IEEE Access
Multidisciplinary | Rapid Review | Open Access Journal

Received June 1, 2018, accepted July 11, 2018, date of publication July 23, 2018, date of current version August 15, 2018.

Digital Object Identifier 10.1109/ACCESS.2018.2858275

A Novel Wideband Filtering Power Divider With Embedding Three-Line Coupled Structures

XI YU, (Student Member, IEEE), AND SHENG SUN, (Senior Member, IEEE)
School of Electronic Science and Engineering, University of Electronic Science and Technology of China, Chengdu 611731, China

Corresponding author: Sheng Sun (sunsheng@ieee.org)

This work was supported in part by the National Natural Science Foundation of China under Grant 61721001 and Grant 61622106, and in part by the Sichuan Science and Technology Program under Grant 2018RZ0142.

ABSTRACT This paper presents a novel wideband filtering power divider. Instead of the T-junction in the traditional power divider design, a three coupled-line structure is utilized to provide the equal power division to every outputs. Together with the quarter-wavelength coupled line in each way, a wideband filtering response can be obtained. In order to enhance the frequency selectivity, a pair of half-wavelength open stubs are loaded between the three-line coupled structure and parallel coupled lines to produce a pair of transmission zeros on both sides of the passband. To enhance the upper stopband rejection, two additional open stubs are installed at output ports. A new three-port equivalent network for the three-line coupled structure is proposed, and the circuit model for the filtering power divider can be developed for illustrating the working mechanism and the design process. Furthermore, the generalized Chebyshev function is applied to synthesize and analyze the whole structure systematically. For demonstration, a prototype of the wideband filtering power divider operating at 3 GHz is designed and fabricated. The measured results show a 16-dB bandwidth of 62%, an isolation better than 16.5 dB, and a 29-dB wide stopband from 4.39 to 7.73 GHz ($1.1f_0$).

INDEX TERMS Wideband, filtering power divider, coupled line, three-line coupled structure, three-port network.

I. INTRODUCTION

As the increasing of demand for the low cost and miniaturization in the wireless communication systems, the RF and microwave components have been developing towards the high integration and multi-function. The filtering power divider which possess both characteristics of frequency selectivity and power division/combination has attracted more and more attention in recent years.

Nowadays, many efforts have been made on exploring the approach to synthesize and design power divider with filtering response. The coupling matrix and J/K inverter as the commonly used techniques for the filter synthesis can be applied to the filtering power divider design [1], [2]. The technique of coupling matrix was adopted to realize the filtering power divider based on folded net-type resonators [1]. However, the frequency selectivity is unsatisfactory, since the number of the resonators is not enough and no cross couplings exist. In order to produce transmission zeros and provide arbitrary coupling coefficient, a dual-path coupling structure was proposed as a K inverter [2]. For the circuit miniaturization, dual-mode resonators [3], [4] and quarter-mode substrate integrated waveguide (SIW) cavity resonators [5] were utilized to reduce the size. Additionally, the discriminating coupling structure [6], short-circuited half-wavelength resonators [7] as well as the mixed electric and magnetic coupling structure [8] were applied to suppress the harmonic signal and achieve a wide upper stopband of the filtering power divider. However, the bandwidth of the filtering power divider mentioned above is narrow. For the wideband application, the multi-mode resonator [9] and ring resonator [10] were embedded to the power divider. By utilizing the first few resonant modes, a wide bandwidth can be achieved. Although an ultra-wideband response could be realized by integrating the hybrid-slotline-to-microstrip-line transition with the Wilkinson power divider [11] or embedding transversal signal-interference sections [12], the out-of-band rejection is not satisfactory. As one of basic structures of the filter, the coupled line is often embedded to the power divider to achieve a wideband response since it can not only offer the desired coupling but also achieve filtering

performance [13]–[16]. By cascading multiple coupled line sections and loading some open/short stubs [13], [14], a wide bandwidth and an upper stopband suppression can be realized, though the DC power cannot be isolated. When coupled lines were installed at each ports [15] or applied to replace the quarter-wavelength transmission lines in the conventional Wilkinson power divider [16], the complete DC isolation and good port matching can be achieved.

However, these filtering power divider with embedded coupled lines are still based on the Wilkinson topology. In order to achieve a more compact structure and enough coupling with a wide range, the three-line coupled structure was adopted in the power divider design [17]–[21], as well as the wideband filter design [22]–[24]. There are three fundamental propagation modes (even-even, odd-odd, and even-odd mode or A, B, and C mode) in the three coupled lines, which have been studied in [25]–[27]. Based on the three propagation modes, three way power divider can be designed by terminating two output ports of the three coupled line with matching load [17], [18]. In addition, a wideband power divider was implemented by shorting the center-line and connecting two side-lines with isolation resistor [19]. In order to achieve filtering response, two transmission zeros at the lower/upper stopband and one in-band transmission zero which splits the wideband passband into two passband can be produced by loading open stubs at the terminal of the three coupled line [20]. By embedding the three-line coupled structure in each way of the two-way Wilkinson topology, a four-way filtering power divider was designed in [21].

In this paper, a novel wideband filtering power divider with an embedding symmetric three-line coupled structure is proposed. Different from the traditional Wilkinson structure, the three-coupled line is used to realize the power division and filtering response instead of the T-junction. An additional coupled-line section is employed to each way of the power divider, which can excite more resonate modes and improve the in-band response. Between the three-line coupled structure and the coupled-line section, a long open stub is inserted to produce two transmission zeros on both sides of the passband to enhance the roll-off skirt. Since there are three propagation modes to describe the characteristics of the three-line coupled structure, the traditional virtual open/short wall at the symmetry plane cannot be directly applied to fully analyze and model this structure. Therefore, a three-port equivalent circuit is proposed to model the three-line coupled structure for the first time. The elements of the three-port equivalent circuit can be derived according to the characteristic impedances of the three modes. Based on the three-port equivalent network, the circuit of the wideband filtering power divider can be built to facilitate the design process. In order to obtain the wideband filtering response with transmission zeros, the generalized Chebyshev function is applied to approximate the characteristic function of the power divider. Finally, all the design parameters can be obtained. For the verification, a prototype of the wideband filtering power divider is designed, fabricated and measured at the center frequency of 3 GHz. The measured results have good agreement with the simulated ones.

II. MODELING OF THE THREE-LINE COUPLED STRUCTURE

Fig. 1 shows the configuration of the six-port three-line coupled structure (Line 1, Line 2, and Line 3) with an electrical length of θ. The three-line coupled structure is symmetric about Line 2. Considering the Yamamoto's condition [25], the static capacitor (conductor to ground) of the centerline is twice as the capacitor of the sidelines, and there are five characteristic mode impedances, of which three are independent. Therefore, in this work, the width of the Line 2 is about twice of the Line 1 and 3 based on Yamamoto's condition [25]. Then, the impedance matrix of the six-port network can be written as

$$\begin{bmatrix} V_1 \\ \vdots \\ V_5 \\ V_6 \end{bmatrix} = \begin{bmatrix} Z_{11} & \cdots & Z_{15} & Z_{16} \\ \vdots & \ddots & Z_{25} & Z_{26} \\ Z_{51} & \cdots & Z_{55} & Z_{56} \\ Z_{61} & \cdots & Z_{65} & Z_{66} \end{bmatrix} \begin{bmatrix} I_1 \\ \vdots \\ I_5 \\ I_6 \end{bmatrix} \tag{1}$$

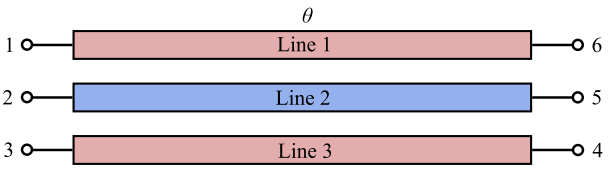

FIGURE 1. Configuration of the three-line coupled structure.

where V_i and I_i are the voltages and currents imposed on port i. Z_{ij} is the impedance parameters associated with port i and j. $(i, j = 1, \cdots 5, 6)$

For the power divider design, port 2 is defined as the input port, and port 4 and 6 are regarded as the output port. Therefore, there are 3 ports left to be applied the open boundary condition. By letting $I_1 = I_3 = I_5 = 0$, (1) can be simplified as

$$\begin{bmatrix} V_2 \\ V_4 \\ V_6 \end{bmatrix} = \begin{bmatrix} Z_{22} & Z_{24} & Z_{26} \\ Z_{42} & Z_{44} & Z_{46} \\ Z_{62} & Z_{64} & Z_{66} \end{bmatrix} \begin{bmatrix} I_2 \\ I_4 \\ I_6 \end{bmatrix} \tag{2}$$

According to the symmetry of this structure, the relationships of $Z_{24} = Z_{26} = Z_{42} = Z_{62}$, $Z_{46} = Z_{64}$, and $Z_{44} = Z_{66}$ can be obtained. After the rearrangement of the port number as shown in Fig. 2, the impedance matrix of the three-port

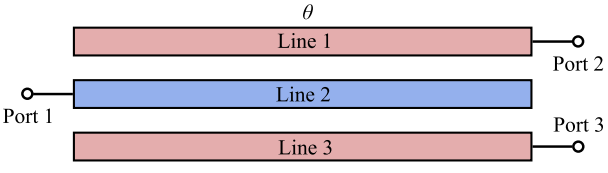

FIGURE 2. Schematic of the three-line coupled structure for the wideband filtering power divider design.

network normalized by Z_0 can be further written as [25]

$$\begin{bmatrix} V'_1 \\ V'_2 \\ V'_3 \end{bmatrix} = \begin{bmatrix} qa & rb & rb \\ rb & pa & ta \\ rb & ta & pa \end{bmatrix} \begin{bmatrix} I'_1 \\ I'_2 \\ I'_3 \end{bmatrix} \tag{3}$$

where

$$q = (z_{2ee} + z_{2oo})/2 \tag{4a}$$
$$r = (z_{2ee} - z_{2oo})/2 \tag{4b}$$
$$p = (z_{2ee} + z_{2oo} + z_{1oe})/2 \tag{4c}$$
$$t = (z_{2ee} + z_{2oo} - z_{1oe})/2 \tag{4d}$$
$$a = -j\cot\theta \quad b = -j\csc\theta \tag{4e}$$

z_{nm} is the normalized characteristic impedance of the n^{th} line at m mode (m denotes ee, oo, or oe). V'_i and I'_i are the voltage and current at i^{th} port ($i = 1, 2, 3$). Fig. 3 shows the three-port network for the three-line coupled structure. Due to the symmetric structure and Yamamoto's condition [25], $z_{1ee} = z_{3ee} = 2z_{2ee}$, $z_{1oo} = z_{3oo} = 2z_{2oo}$, and $z_{1oe} = z_{3oe}$. Therefore, the impedance matrix of the three coupled line structure can be represented by only three characteristic mode impedances z_{2ee}, z_{2oo}, and z_{1oe}.

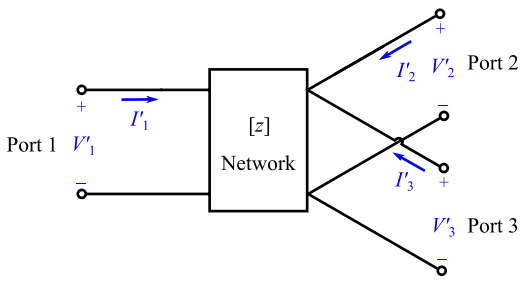

FIGURE 3. Three-port network for three-line coupled structure.

By utilizing the Richard' transformation $s = j\tan\theta$, the normalized impedance matrix can be presented as

$$[z] = \frac{1}{s}\begin{bmatrix} q & r\sqrt{1-s^2} & r\sqrt{1-s^2} \\ r\sqrt{1-s^2} & p & t \\ r\sqrt{1-s^2} & t & p \end{bmatrix} \tag{5}$$

In this work, a simple star-shaped three-port network is adopted to be equivalent to the three-line coupled structure. From (5), it can be found that z_{12} and z_{13} have the term of $\sqrt{1-s^2}/s$, however, z_{23} is only related to $1/s$. As is well known, the mutual impedance of the unit element is associated with $\sqrt{1-s^2}/s$, and self-impedance is associated with $1/s$. Therefore, there must be one unit element between port 1 and port 2 (3). Moreover, the unit element should not exist at the direct path between port 2 and port 3, since z_{23} is not related to $\sqrt{1-s^2}/s$.

Based on the impedance matrix of the three-line coupled structure, the new three-port equivalent circuit under s domain ($s = j\tan\theta$) is derived as shown in Fig. 4. The equivalent circuit consists of a unit element and three capacitances.

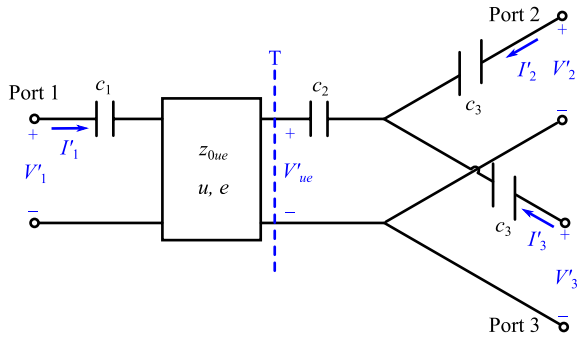

FIGURE 4. The proposed three-port equivalent circuit for the three-line coupled structure under $s = j\tan\theta$ domain.

The impedance parameters of this equivalent circuit can be calculated as

$$z_{c11} = \left.\frac{V'_1}{I'_1}\right|_{I'_2=I'_3=0} = \frac{1}{sc_1} + \frac{z_{0ue}}{s} \tag{6a}$$
$$z_{c12} = \left.\frac{V'_1}{I'_2}\right|_{I'_1=I'_3=0} = \frac{V'_{ue} - sz_{0ue}I'_2}{\sqrt{1-s^2}I'_2} = z_{0ue}\sqrt{1-s^2} \tag{6b}$$
$$z_{c22} = \left.\frac{V'_2}{I'_2}\right|_{I'_1=I'_3=0} = \frac{1}{sc_2} + \frac{1}{sc_3} + \frac{z_{0ue}}{s} \tag{6c}$$
$$z_{c23} = \left.\frac{V'_2}{I'_3}\right|_{I'_1=I'_2=0} = \frac{1}{sc_2} + \frac{z_{0ue}}{s} \tag{6d}$$

where $V'_{u,e}$ are the voltage of the unit element at reference plane T.

By solving the equation $z_{c11} = z_{11}$, $z_{c12} = z_{12}$, $z_{c22} = z_{22}$, and $z_{c23} = z_{23}$, the impedance of the unit element and the values of capacitors can be extracted as

$$z_{0ue} = r = \frac{z_{2ee} - z_{2oo}}{2} \tag{7a}$$
$$c_1 = \frac{1}{q-r} = \frac{1}{z_{2oo}} \tag{7b}$$
$$c_2 = \frac{1}{t-r} = \frac{2}{2z_{2oo} - z_{1oe}} \tag{7c}$$
$$c_3 = \frac{1}{p-t} = \frac{1}{z_{1oe}} \tag{7d}$$

When port 1 is short ended or port 2 (3) is open ended, the two-port network degenerated from the three-port network is the same as the one in [25], which validates the correctness of the proposed three-port network. Since the elements in the three-port network are correlated with the three propagation mode impedances, the proposed three-port network can be utilized to accurately depict the characteristics of the three-line coupled structure.

III. WIDEBAND FILTERING POWER DIVIDER DESIGN AND ANALYSIS

A. SYNTHESIS OF THE FILTERING POWER DIVIDER

Fig. 5 illustrates the circuit configuration of the proposed wideband filtering power divider. It consists of a three-line

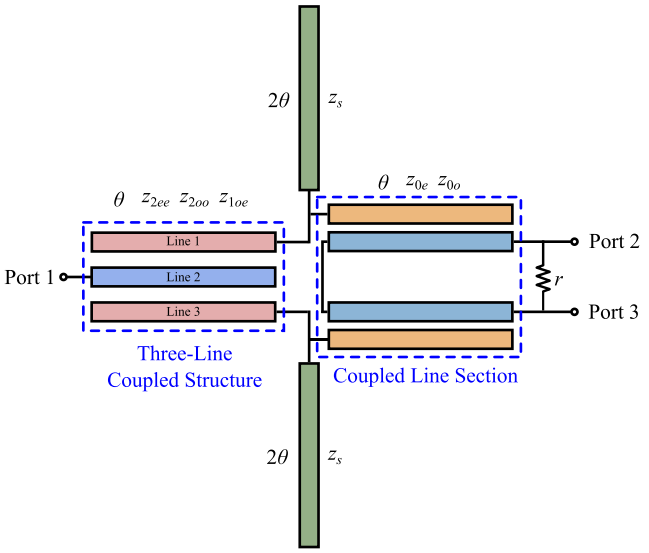

FIGURE 5. The schematic diagram of the proposed wideband filtering power divider.

coupled structure, two coupled line structures and two long open stubs. The center-line of the three-line coupled structure is regarded as the input port to provide the coupling to each way of the filtering power divider. The open stubs are inserted between the three-line coupled structure and the coupled lines. Besides, a resistor r is connected between two output ports to improve the isolation. z_s and z_{0e}, z_{0o} are the normalized characteristic impedances of the open stubs and the normalized even-odd mode impedances of the coupled lines, respectively, while the electrical length θ is chosen as $\theta_0 = \pi/2$, which is quarter-wavelength at the center operating frequency f_0. For simplicity, the phase velocities of the even and odd modes are assumed to be the same so that the coupled line sections have the same even/odd-mode electrical length.

Due to the symmetric structure, the even-odd mode theory is considered to analyze the filtering power divider. However, since the three-line coupled structure has three propagation modes, traditional even-odd mode theory cannot be directly applied to analyze its characteristics in physical structure. Thus, the proposed three-port equivalent network are used to represent the three-line coupled structure during the even-odd mode analysis. Under the even and odd mode excitation, the proposed filtering power divider can be decomposed into two half circuit models as shown in Fig. 6. When even mode is excited, the equivalent half circuit model is built under s domain as shown in Fig. 6 (a). It consists of two unit elements, five capacitances, and one inductor. The values of these elements are derived as

$$z_{01} = z_{2ee} - z_{2oo} \quad z_{02} = \frac{z_{0e} - z_{0o}}{2} \tag{8a}$$

$$c_{e1} = \frac{1}{2z_{2oo}} \quad c_{e2} = \frac{1}{z_{0o}} \quad c_{e3} = \frac{2}{z_s} \tag{8b}$$

$$l_e = \frac{z_s}{2} \tag{8c}$$

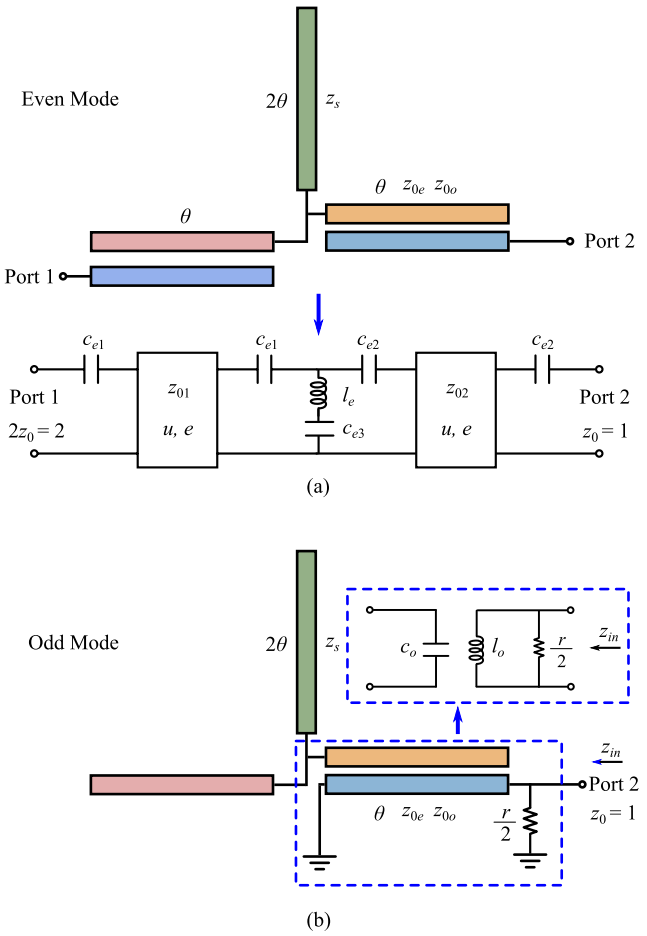

FIGURE 6. The decomposed half circuit model of the proposed wideband filtering power divider under s plane. (a) Even-mode half circuit model. (b) Odd-mode half circuit model.

It can be found that z_{1oe} is coincidently eliminated during the circuit simplification and a symmetric two-port network are obtained with z_{2ee} and z_{2oo}, which is degraded from the three-port network. On the other hand, when odd mode is excited, the parallel coupled-line section is loaded with short circuited and open circuited termination, of which the frequency response is all-stop. Its equivalent circuit is shown in Fig. 6 (b). The values of c_o and l_o are

$$c_o = \frac{2}{z_{0e} + z_{0o}} \quad l_o = \frac{z_{0e} + z_{0o}}{2} \tag{9}$$

Then, the S-parameters $[S_e]$ of two-port even-mode circuit and $[S_o]$ of single-port odd-mode circuit can be obtained by using the following relationships respectively

$$S_{e11} = \frac{A_e + B_e - 2C_e - 2D_e}{A_e + B_e + 2C_e + 2D_e} \tag{10a}$$

$$S_{e21} = \frac{2\sqrt{2}}{A_e + B_e + 2C_e + 2D_e} \tag{10b}$$

$$S_{e22} = \frac{-A_e + B_e - 2C_e + 2D_e}{A_e + B_e + 2C_e + 2D_e} \tag{10c}$$

$$S_{o22} = \frac{z_{in} - 1}{z_{in} + 1} \tag{10d}$$

where

$$z_{in} = \frac{r\left(z_{0e} + z_{0o}\right)s}{2r + 2\left(z_{0e} + z_{0o}\right)s} \tag{11}$$

A_e, B_e, C_e, and D_e are the elements in the $ABCD$-matrix of the even-mode half circuit model. Based on $[S_e]$ and $[S_o]$, the S-parameters $[S]$ of the filtering power divider can be given as

$$S_{11} = S_{e11} \tag{12a}$$
$$S_{21} = S_{31} = \frac{S_{e21}}{\sqrt{2}} \tag{12b}$$
$$S_{22} = S_{33} = \frac{S_{e22} + S_{o22}}{2} \tag{12c}$$
$$S_{23} = \frac{S_{e22} - S_{o22}}{2} \tag{12d}$$

By using the relationship of $F_{PD} = S_{11}/S_{21}$, the characteristic function F_{PD} of the filtering power divider can be derived as

$$F_{PD}(s) = \frac{k_1 s^5 + k_2 s^4 + k_3 s^3 + k_4 s^2 + k_5 s + k_6}{k_7 s\left(s^4 - 1\right)} \tag{13}$$

where k_1 to k_7 as function of z_{2ee}, z_{2oo}, z_{0e}, z_{0o} and z_s are given in the Appendix. By letting the denominator equals to zero, the transmission zeros of the filtering power divider in s domain can be solved as

$$s_z = \left\{0 \quad -1 \quad 1 \quad -j \quad j\right\} \tag{14}$$

In order to achieve in-band equal ripple response with the prescribed bandwidth, the generalized Chebyshev function can be utilized to synthesize the in-band performance of the filters, which has been discussed in [28]–[30]. For the power divider application, the characteristic function with Chebyshev response in the normalized low-pass domain Ω can be expressed as

$$F_N(\Omega) = \sqrt{2}\varepsilon j\frac{F(\Omega)}{P(\Omega)} = \sqrt{2}\varepsilon j\cosh\left[\sum_{n=1}^{N}\cosh^{-1}\left(\Omega_n\right)\right] \tag{15}$$

where

$$\Omega_n = \frac{\Omega - 1/\Omega_{zn}}{1 - \Omega/\Omega_{zn}} \quad \varepsilon = \frac{1}{\sqrt{10^{RL/10} - 1}} \tag{16}$$

$F(\Omega)$ and $P(\Omega)$ are the reflection and transmission polynomials of the filtering power divider. Herein, Ω_{zn} is the n^{th} normalized transmission zeros and ε is the in-band equal-ripple constant in related with the return loss RL (dB). By using the frequency mapping function [28]

$$\Omega = -\frac{\delta}{\tan\theta} = -j\frac{\delta}{s} \quad \delta = \frac{1}{\tan\left(\frac{\pi}{4}\cdot FBW\right)} \tag{17}$$

the bandpass prototype (s domain) can be transformed to the normalized low-pass prototype (Ω domain). Then, after the normalization, the transmission zeros in Ω domain are

$$\Omega_z = \delta\cdot\left\{\inf \quad -j \quad j \quad -1 \quad 1\right\} \tag{18}$$

From (18), it can be found that there two real frequency transmission zeros, two imaginary frequency transmission zeros, and only one transmission zero at infinite. If the order of the Chebyshev function is N, the maximum number of the achievable transmission zeros (including imaginary and infinite frequency) is also N. Since the degree of the numerator of F_{PD} is no more than five and the number of the transmission zeros is totally five, the proposed power divider can achieve fifth order filtering response. Therefore, when $N = 5$, the reflection and transmission polynomials can be derived by using the recursive technique [31]

$$P(\Omega) = -\frac{\Omega^4}{\delta^4} + 1 \tag{19a}$$
$$F(\Omega) = h_1\Omega^5 + h_2\Omega^3 + h_3\Omega \tag{19b}$$

where

$$h_1 = \left(2 + 2\sqrt{1 + \frac{1}{\delta^2}} + \frac{1}{\delta^2}\right)\left(2 + 2\sqrt{1 - \frac{1}{\delta^2}} - \frac{1}{\delta^2}\right) \tag{20}$$

$$h_2 = \left(\frac{2}{\delta^2} - 6\right)\sqrt{1 + \frac{1}{\delta^2}} - \left(\frac{2}{\delta^2} + 6\right)\sqrt{1 - \frac{1}{\delta^2}} - 4\sqrt{1 - \frac{1}{\delta^4}} - 4 \tag{21}$$

$$h_3 = 2\sqrt{1 + \frac{1}{\delta^2}} + 2\sqrt{1 - \frac{1}{\delta^2}} + 1 \tag{22}$$

Substitute (19a) and (19b) into (15), the characteristic function of filtering power divider with Chebyshev response can be obtained

$$F_N(\Omega) = \sqrt{2}\varepsilon\delta^4 j\frac{h_1\Omega^5 + h_2\Omega^3 + h_3\Omega}{-\Omega^4 + \delta^4} \tag{23}$$

After the frequency transformation, the characteristic function in s domain is exhibited as

$$F_N(s) = \sqrt{2}\varepsilon\frac{\delta h_3 s^4 - \delta^3 h_2 s^2 + \delta^5 h_1}{s^5 - s} \tag{24}$$

Let $F_{PD} = F_N$, the following relationships are acquired

$$k_1 = k_3 = k_5 = 0 \tag{25a}$$
$$k_7 = 1 \tag{25b}$$
$$k_2 = \sqrt{2}\varepsilon\delta h_3 \tag{25c}$$
$$k_4 = -\sqrt{2}\varepsilon\delta^3 h_2 \tag{25d}$$
$$k_6 = \sqrt{2}\varepsilon\delta^5 h_1 \tag{25e}$$

Based on the equations above, z_{2ee}, z_{2oo}, z_{0e}, z_{0o} and z_s can be calculated. Besides, the relationship among z_{2ee}, z_{2oo}, z_{0e}, and z_{0o} can be also obtained.

$$(z_{2ee} - z_{2oo})^2 = \frac{1}{2}(z_{0e} - z_{0o})^2 \tag{26}$$

Then, according to the distribution of the capacitors in the substrate with a dielectric constant of ϵ_r under the three

propagation modes [17], the relationships between z_{1eo} and z_{2ee}, z_{2oo} can be obtained as follows

$$z_{1oe} = \frac{2\,(1+\varepsilon_r)\,z_{2ee}z_{2oo}}{2\varepsilon_r z_{2oo} + (1+\varepsilon_r)\,z_{2ee}} \tag{27}$$

In order to achieve a good in-band isolation, a resistor is loaded and determined by solving $S_{23} = 0$ at the operating center frequency. By using (26), the isolation resistor r is calculated and simplified as

$$r = \frac{(z_{0e} - z_{0o})^2}{(z_{2ee} - z_{2oo})^2} = 2 \tag{28}$$

Then, the wideband filtering power divider can be designed by de-normalizing z_{2ee}, z_{2oo}, z_{1oe}, z_{0e}, z_{0o}, z_s, r and mapping all of the design parameters into the physical dimension [18], [25].

B. DISCUSSION AND ANALYSIS

After all the parameters of the proposed filtering power divider are determined, the frequency response can be theoretically calculated according to (12a)-(12d). Fig. 7 shows the calculated frequency response of the wideband filtering power divider under the normalized frequency with typical parameters. It can be observed that there two transmission zeros at each sides of the passband. The two transmission zeros near the passband are produced by the loaded open stubs and the other two are introduced by the coupled line structures. The return loss of input/output port and in-band isolation are all below -20 dB. Fig. 8 illustrates the effects of z_s on the in-band response. When z_s equals to 0.7, equi-ripple response can be achieved and there are totally five transmission poles in the passband. When z_s is small, the two poles off the center frequency can merge into one pole. If z_s is larger than 0.7, $|S_{11}|$ are deteriorated near the edge frequency of the passband while the bandwidth is increased. As z_s increases gradually, the reflection at port 2/3 is slight improved and in-band $|S_{22(33)}|$ is below -20 dB. However, the in-band performance of $|S_{23}|$ are deteriorated.

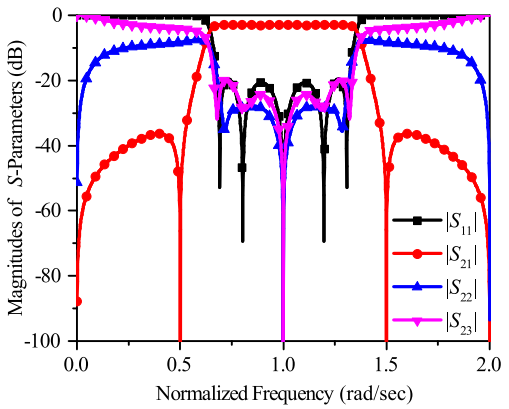

FIGURE 7. The calculated theoretical *S*-parameters of the wideband filtering power divider under the normalized frequency. ($z_{0e} = 3.04$, $z_{0o} = 1.19$, $z_{2ee} = 2.15$, $z_{2oo} = 0.84$, and $z_s = 0.70$).

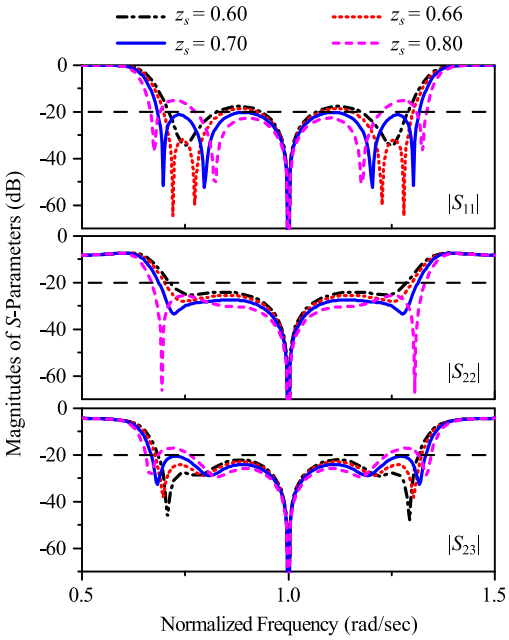

FIGURE 8. The *S*-parameters of the wideband filtering power divider with different z_s

The synthesized curve for the in-band equi-ripple response is depicted in Fig. 9 for a quick design process. Fig. 9 (a) shows the values of z_{0e}, z_{0o}, z_{2ee}, z_{2oo}, and z_s versus the bandwidth of impedance and isolation. As z_{0e}, z_{0o}, z_{2ee}, z_{2oo} decrease and z_s increases gradually, the bandwidths for both impedance and isolation increase. Under the same impedance parameters, the isolation bandwidth is slightly wider than the impedance bandwidth. Considering that the coupling factor CF of the coupled line structure is between -5 dB and -10 dB ($CF = -20\log[(z_{0e} - z_{0o})/(z_{0e} + z_{0o})]$), and the achievable impedance range for microstrip line is between 20 and 150 Ω, the bandwidth of the proposed filtering power divider can be realized from 50% to 80%. Moreover, the relationships between the rejection/isolation and the impedance bandwidth can be found in Fig. 9 (b). The performance of the in-band isolation and out-of-band rejection become better with the decrease of the bandwidth. Therefore, there is a trade-off between the bandwidth and the rejection/isolation. The frequency responses of the three cases marked as A, B, and C in Fig. 9 are plotted in Fig. 10 (a) and (b). Fig. 10 directly demonstrates the control of the power division bandwidth with different impedance parameters. Case C has a wider bandwidth and a sharp roll-off skirt, although the out-of-band rejection level and the in-band isolation is unsatisfactory compared with the others. For the Case A, the bandwidth is narrower than Case B and C with high even-odd mode impedances and low characteristic impedance of the open stub (z_s).

C. HARMONIC SUPPRESSION

A filtering power divider with $z_{0e} = 3.04$, $z_{0o} = 1.19$, $z_{2ee} = 2.15$, $z_{2oo} = 0.84$, $z_{1oe} = 1.04$, $z_s = 0.70$, and $r = 2$ is designed at the operating center frequency of $f_0 = 3$ GHz.

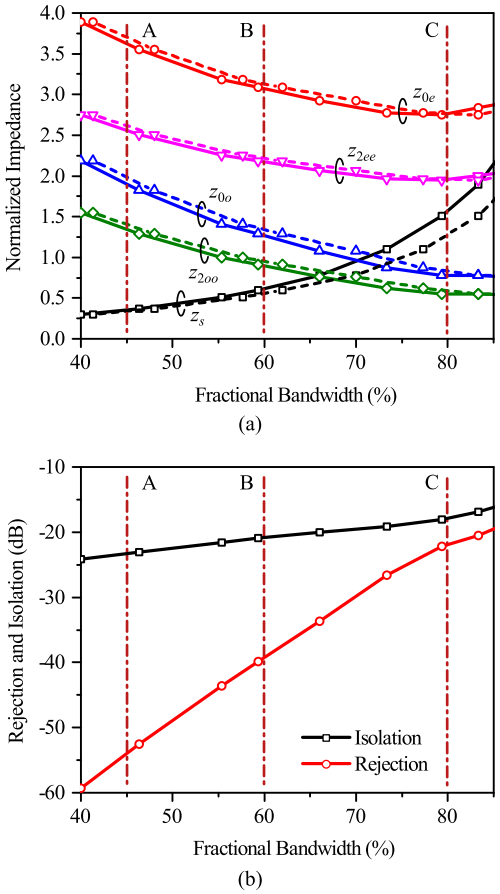

FIGURE 9. (a) The impedances of the proposed filtering power divider versus fractional bandwidth. (impedance bandwidth: solid line; isolation bandwidth: dash line). (b) The in-band isolation and out-of-band rejection versus fractional bandwidth.

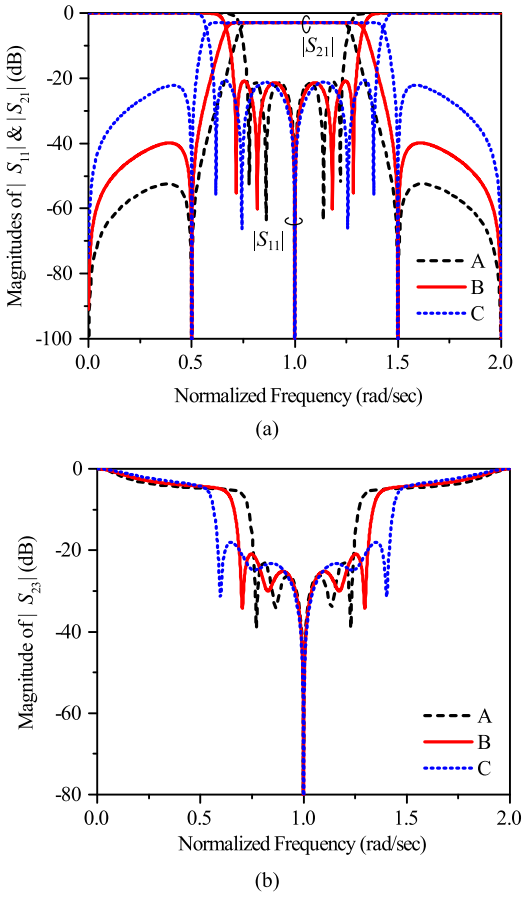

FIGURE 10. The magnitudes of S-parameters for case A, B and C marked in Fig. 9. (a) The magnitudes of $|S_{11}|$ and $|S_{21}|$. (b) The magnitude of $|S_{23}|$.

The substrate is RO4350B with a thickness of 0.508 mm and a dielectric constant of 3.66. The circuit simulated results are curved by dash line as shown in Fig. 11. It can be found that there are two transmission zeros at two sides of the pass-band and the complete DC isolation is achieved. However, a strong second harmonic of f_0 is generated at 6 GHz since the even- and odd-mode phase velocities of the coupled line are actually unequal. In order to suppress the harmonic and broaden the upper stopband, an open stub are loaded at each output ports. When the electrical length of the stub is chosen as $\theta_0/2$, an additional transmission zero is produced at $2f_0$ to suppress the spurious frequency as shown in Fig. 11 curved by solid line. Due to the loaded open stub, an capacitive element is introduced at the output port. In order to remain the good in-band isolation, an inductor is in series with the isolation resistor to compensate the capacitive effect. Fig. 12 shows the half circuit model with open stub under the odd-mode excitation. According to its equivalent circuit, the input impedance z'_{in} can be calculated as

$$z'_{in} = \frac{1}{\frac{2}{r+j\omega l} + \frac{2}{j(z_{0e}+z_{0o})\tan\theta_0} + \frac{1}{z_x}} \tag{29}$$

where $z_x = -jz_{os}\cot\frac{\theta_0}{2}$. Substitute z'_{in} into (10d), S_{o22} can be determined. Then, by solving $S_{23} = 0$ and using the

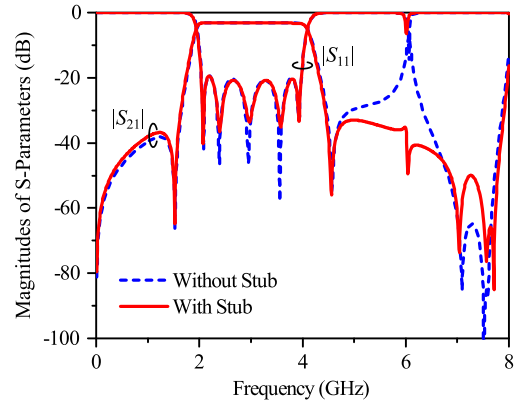

FIGURE 11. The circuit simulated frequency responses of the filtering power divider with (solid line) and without (dash line) open stub for the harmonic suppression.

relationship of (26), the resistor and inductor are obtained and simplified as

$$r = \frac{2z_{os}^2}{1+z_{os}^2} \tag{30a}$$

$$l = \frac{z_{os}}{(1+z_{os}^2)\,\pi f_0} \tag{30b}$$

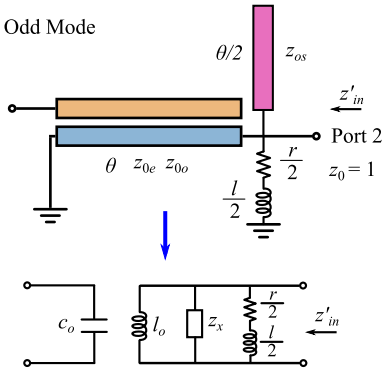

FIGURE 12. The decomposed odd-mode half circuit model with open stub and its equivalent circuit.

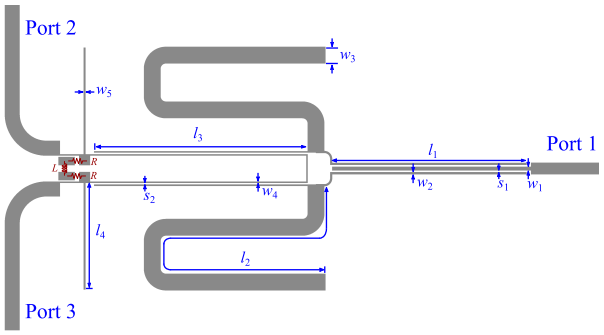

FIGURE 13. The layout of the wideband filtering power divider with physical-dimension definitions.

D. DESIGN PROCEDURES

According to the above theoretical synthesis and analysis, the design procedures for the proposed wideband filtering power divider with harmonic suppression are summarized as follows:

1) Determine the operating center frequency f_0, return loss RL, fractional bandwidth FBW, and the dielectric constant ϵ_r of the substrate.
2) Under the normalized frequency and impedance, synthesize the initial wideband filtering power divider according to the pre-determined specifications. Obtain the normalized design parameters z_{2ee}, z_{2oo}, z_{1oe}, z_{0e}, z_{0o} and z_s.
3) Choose a proper value z_{os} of short open stubs at output ports for the harmonic suppression. Calculate the values of the isolation resistor r and inductor l. Then, the final design parameters can be obtained after some optimization.
4) De-normalize the design parameters z_{2ee}, z_{2oo}, z_{1oe}, z_{0e}, z_{0o}, z_s, z_{os}, r, and l by $Z_0 = 50\ \Omega$. Finally, map them into the physical structure.

IV. IMPLEMENTATION AND RESULTS

In order to validate the proposed design theory, a prototype of the wideband filtering power divider is finally designed, fabricated, and measured at the operating center frequency of 3 GHz. The pre-determined specifications of the filtering power divider are $RL = 20$ dB, $f_0 = 3$ GHz, $FBW = 2/3$, and $Z_0 = 50\ \Omega$. The substrate is still RO4350B aforementioned. According to the design procedures, the final de-normalized design parameters can be obtained as $\theta = \theta_0 = 90°$, $Z_s = 46\ \Omega$, $Z_{os} = 120\ \Omega$, $Z_{0e} = 186\ \Omega$, $Z_{0o} = 65\ \Omega$, $Z_{2ee} = 131\ \Omega$, $Z_{2oo} = 46\ \Omega$, $Z_{1oe} = Z_{3oe} = 59\ \Omega$, $Z_{1ee} = Z_{3ee} = 262\ \Omega$, $Z_{1oo} = Z_{3oo} = 92\ \Omega$, $R = 45\ \Omega$, and $L = 1.7$ nH. The layout of the proposed wideband filtering power divider with physical-dimension definitions and the photograph of the fabricated one are depicted in Fig. 13 and Fig. 14 (a), respectively. The corresponding dimensions are as follows: $w_1 = 0.28$, $w_2 = 0.15$, $w_3 = 1.22$, $w_4 = 0.10$, $w_5 = 0.14$, $l_1 = 14.25$, $l_2 = 30.41$, $l_3 = 15.65$, $l_4 = 7.8$, $s_1 = 0.13$, and $s_2 = 0.12$ (units: mm).

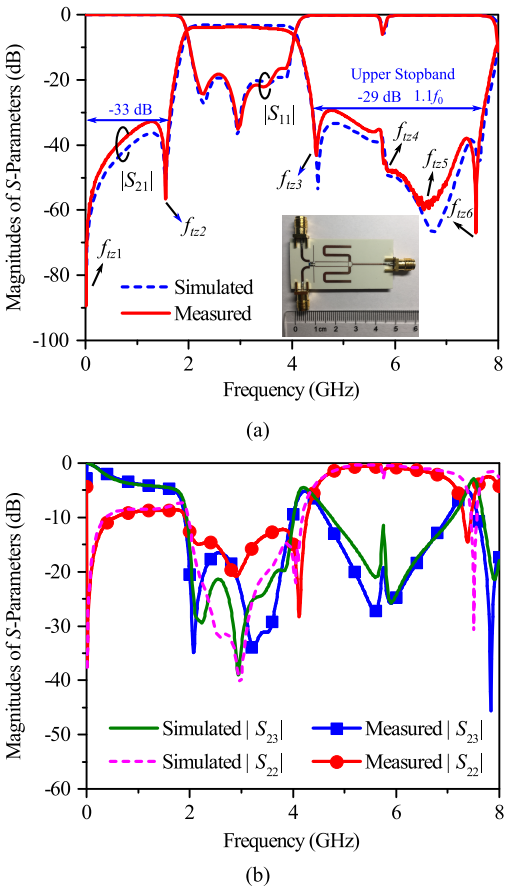

FIGURE 14. The EM simulated and measured results of the proposed wideband filtering power divider. (a) The magnitudes of $|S_{11}|$ and $|S_{21}|$ (Inset: photograph of the fabricated filtering power divider). (b) The magnitudes of $|S_{22}|$ and $|S_{23}|$.

Fig. 14 illustrates the full-wave simulated and measured results of the wideband filtering power divider. Within the passband, the return loss is better than 16 dB and the minimum insertion loss is about -3-0.6 dB. The measured fractional bandwidth of 16-dB in-band return loss is about 62%

TABLE 1. Comprison between the previous designs and this design.

Reference	Filtering Response	DC Isolation	f_0 (GHz)	RL[1] (dB)	FBW (In-band) (%)	Rejection (dB)	BW (Stopband) (GHz)	IL[2] (In-band) (dB)	Isolation (dB)	TZs[3]
[9]	Yes	Yes	2.3	17	31	20	$4.2f_0$	4.3	17	2
[10]	Yes	Yes	2.05	10	62	15.8	$0.95f_0$	-	10	5
[11]	No	Yes	6.8	15	85.3	-	-	4	15	-
[12]	Yes	No	3	15	90	26	$0.4f_0$	-	17	4
[13]	Yes	No	3	15	104.5	17.2	$3.4f_0$	3.7	15	3
[14]	Yes	No	1	20	43	20	$3.9f_0$	3.2	20	5
[15]	No	Yes	2	15	62	-	-	-	20	-
[16]	Yes	Yes	3	15	70	13	$1.1f_0$	3.3	16.7	4
This Design	Yes	Yes	3	16	62	29	$1.1f_0$	3.6	16.5	6

RL[1]: Return Loss; IL[2]: Insertion Loss; TZs[3]: Transmission Zeros

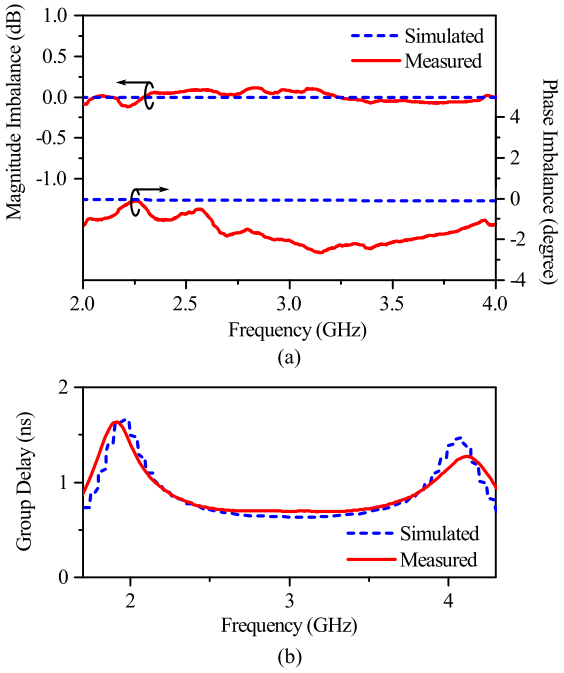

FIGURE 15. (a) The in-band magnitude and phase imbalance. (b) The group delay of the filtering power divider.

over the frequency range from 2.08 to 3.95 GHz. The in-band isolation between two output ports is better than 16.5 dB with a 64% isolation bandwidth from 1.97 to 3.84 GHz. Moreover, a 33-dB rejection is achieved at the lower stopband and a 29-dB harmonic suppression is achieved at the upper stopband from 4.39 to 7.73 GHz, which is about $1.1f_0$. It can be noticed that there are six transmission zeros over the concerned frequency band. The first transmission zero f_{tz1} is at zero frequency, which means the complete DC isolation. It makes the proposed filtering power divider very suitable for the balanced amplifier designs since it has no requirement of capacitors. The transmission zeros f_{tz2} and f_{tz3} are located at 1.55 GHz and 4.47 GHz, which is introduced by the long open stub, while f_{tz4} introduced by the short open stub is allocated at 5.9 GHz to suppress the second harmonic of f_0. Due to the existing of the coupled lines and the periodic transmission zero generated by the long open stub, two more transmission zeros f_{tz5} and f_{tz6} are introduced at 6.66 GHz and 7.56 GHz. With the help of the four transmission zeros ($f_{tz3}, f_{tz4}, f_{tz5}$, and f_{tz6}) at the upper stopband, the spurious frequencies are well suppressed and a wide stopband is obtained up to 7.73 GHz. As observed from Fig. 15 (a), the magnitude and phase imbalance between two output ports are less than ± 0.11 dB and $\pm 2.65°$, respectively. Fig. 15 (b) shows the in-band group delay of the filtering power divider. The maximum variation of the measured group delay is about 0.71 ns (from 0.69 to 1.4 ns) over the passband (from 2 to 4 GHz). Comparison with the other design in the state of the art is tabulated in Table 1. It can be found that the proposed filtering power divider features a wide bandwidth of 62%, sharp roll-of skirt, high isolation, well spurious frequency rejection of 29 dB, and complete DC isolation.

V. CONCLUSION

Based on the proposed new equivalent circuit of the three-line coupled structure, a circuit model of the wideband filtering power divider has been built. After the systematical study on the filtering response of the power divider with transmission zeros by applying the Chebyshev function, a novel wideband filtering power divider has been synthesized and designed. The measurement of fabrication demonstrates that the design owns a 62% bandwidth, a high 29-dB stopband rejection and an isolation better than 16.5 dB.

APPENDIX

In (13), the coefficients (k_1 to k_7) of the characteristic function F_{PD} correlated with z_{2ee}, z_{2oo}, z_{0e}, z_{0o} and z_s are calculated as

$$k_1 = \left[(z_{2ee} - z_{2oo})^2 - \frac{1}{2}(z_{0e} - z_{0o})^2\right] z_s \tag{A.1}$$

$$k_2 = -\frac{1}{2}(z_{0e} - z_{0o})^2(z_{2ee} - z_{2oo})^2 + \frac{1}{4}z_s\,(z_{2ee} + z_{2oo})(z_{0e} - z_{0o})^2 + \frac{1}{2}z_s\,(z_{0e} - z_{0o})\left[(z_{2ee} - z_{2oo})^2 - 2\right] + z_{0o}(z_{2ee} - z_{2oo})^2 z_s - 2\,(z_{0o} + z_{2ee} + z_{2oo})\,z_s \tag{A.2}$$

$$k_3 = -(z_{0e}+z_{0o})(z_{2ee}-z_{2oo})^2+(z_{0e}-z_{0o})^2 (z_{2ee}+z_{2oo})-\frac{1}{2}(z_{0e}-z_{0o})^2 z_s+(z_{2ee}-z_{2oo})^2 z_s + z_{0o}(z_{2ee}+z_{2oo})z_s-2z_{0o}(z_{0o}+z_{2ee}+z_{2oo})z_s - \frac{1}{2}(z_{0e}-z_{0o})(4z_{0o}+z_{2ee}+z_{2oo})z_s+4z_{2ee}z_{2oo}z_s \tag{A.3}$$

$$k_4 = \frac{1}{4}\left(z_{0e}^2+z_{0o}^2\right)(z_{2oo}z_s-8z_{2ee}z_{2oo}+z_{2ee}z_s)-z_{0e}z_s + \frac{1}{2}z_{0o}\left(4z_{2oo}+4z_{2ee}-2z_s+z_{2ee}^2z_s+z_{2oo}^2z_s\right) + z_{0o}z_{2ee}z_{2oo}z_s+\frac{1}{2}z_{0e}\left(z_{2ee}^2+z_{2oo}^2\right)(z_s-4z_{0o}) + \frac{1}{2}z_{0e}z_{2oo}(4+z_{0o}z_s)-2z_s(z_{2ee}+z_{2oo}) + \frac{1}{2}z_{0e}z_{2ee}(4+2z_{2oo}z_s+16z_{0o}z_{2oo}+z_{0o}z_s) \tag{A.4}$$

$$k_5 = 4z_{0e}[z_{0o}(z_{2ee}+z_{2oo})-z_{2ee}z_{2oo}]+4z_{2ee}z_{2oo}z_s - \frac{1}{2}z_{0o}(8z_{2ee}z_{2oo}+z_{2ee}z_s+z_{2oo}z_s) - \frac{1}{2}z_{0e}z_s(4z_{0o}+z_{2ee}+z_{2oo}) \tag{A.5}$$

$$k_6 = (z_{2ee}+z_{2oo})z_{0e}z_{0o}z_s+2(z_{0e}+z_{0o})z_{2ee}z_{2oo}z_s - 8z_{0e}z_{0o}z_{2ee}z_{2oo} \tag{A.6}$$

$$k_7 = (z_{0e}-z_{0o})(z_{2ee}-z_{2oo})z_s \tag{A.7}$$

REFERENCES

[1] C.-F. Chen and C.-Y. Lin, "Compact microstrip filtering power dividers with good in-band isolation performance," *IEEE Microw. Wireless Compon. Lett.*, vol. 24, no. 1, pp. 17–19, Jan. 2014.

[2] K.-X. Wang, X. Y. Zhang, and B.-J. Hu, "Gysel power divider with arbitrary power ratios and filtering responses using coupling structure," *IEEE Trans. Microw. Theory Techn.*, vol. 62, no. 3, pp. 431–440, Mar. 2014.

[3] G. Zhang, J. Wang, L. Zhu, and W. Wu, "Dual-mode filtering power divider with high passband selectivity and wide upper stopband," *IEEE Microw. Wireless Compon. Lett.*, vol. 27, no. 7, pp. 642–644, Jul. 2017.

[4] G. Zhang, X. Wang, J.-S. Hong, and J. Yang, "A high-performance dual-mode filtering power divider with simple layout," *IEEE Microw. Wireless Compon. Lett.*, vol. 28, no. 2, pp. 120–122, Feb. 2018.

[5] X. Wang and X.-W. Zhu, "Quarter-mode circular cavity substrate integrated waveguide filtering power divider with via-holes perturbation," *Electron. Lett.*, vol. 53, no. 12, pp. 791–793, Aug. 2017.

[6] X.-L. Zhao, L. Gao, X. Y. Zhang, and J.-X. Xu, "Novel filtering power divider with wide stopband using discriminating coupling," *IEEE Microw. Wireless Compon. Lett.*, vol. 26, no. 8, pp. 580–582, Aug. 2016.

[7] W.-M. Chau, K.-W. Hsu, and W.-H. Tu, "Wide-stopband Wilkinson power divider with bandpass response," *Electron. Lett.*, vol. 50, no. 1, pp. 39–40, Jan. 2014.

[8] X. Y. Zhang, K.-X. Wang, and B.-J. Hu, "Compact filtering power divider with enhanced second-harmonic suppression," *IEEE Microw. Wireless Compon. Lett.*, vol. 23, no. 9, pp. 483–485, Sep. 2013.

[9] Y. Deng, J. Wang, and J.-L. Li, "Design of compact wideband filtering power divider with extended isolation and rejection bandwidth," *Electron. Lett.*, vol. 52, no. 16, pp. 1387–1389, Apr. 2016.

[10] S. S. Gao, S. Sun, and S. Xiao, "A novel wideband bandpass power divider with harmonic-suppressed ring resonator," *IEEE Microw. Wireless Compon. Lett.*, vol. 23, no. 3, pp. 119–121, Mar. 2013.

[11] K. Song, Y. Zhu, Q. Duan, M. Fan, and Y. Fan, "Extremely compact ultra-wideband power divider using hybrid slotline/microstrip-line transition," *Electron. Lett.*, vol. 51, no. 24, pp. 2014–2015, Nov. 2015.

[12] L. Jiao, Y. Wu, Y. Liu, Q. Xue, and Z. Ghassemlooy, "Wideband filtering power divider with embedded transversal signal-interference sections," *IEEE Microw. Wireless Compon. Lett.*, vol. 27, no. 12, pp. 1068–1070, Dec. 2017.

[13] C.-W. Tang and J.-T. Chen, "A design of 3-dB wideband microstrip power divider with an ultra-wide isolated frequency band," *IEEE Trans. Microw. Theory Techn.*, vol. 64, no. 6, pp. 1806–1811, Jun. 2016.

[14] Y. Wu, Z. Zhuang, Y. Liu, L. Deng, and Z. Ghassemlooy, "Wideband filtering power divider with ultra-wideband harmonic suppression and isolation," *IEEE Access*, vol. 4, pp. 6876–6882, 2016.

[15] M. A. Maktoomi, M. S. Hashmi, and F. M. Ghannouchi, "Theory and design of a novel wideband DC isolated Wilkinson power divider," *IEEE Microw. Wireless Compon. Lett.*, vol. 26, no. 8, pp. 586–588, Aug. 2016.

[16] B. Zhang and Y. Liu, "Wideband filtering power divider with high selectivity," *Electron. Lett*, vol. 51, no. 23, pp. 1950–1952, Nov. 2015.

[17] A. M. Abbosh, "Three-way parallel-coupled microstrip power divider with ultrawideband performance and equal-power outputs," *IEEE Microw. Wireless Compon. Lett.*, vol. 21, no. 12, pp. 649–651, Dec. 2011.

[18] A. M. Abbosh, "Design of ultra-wideband three-way arbitrary power dividers," *IEEE Trans. Microw. Theory Techn.*, vol. 56, no. 1, pp. 194–201, Jan. 2008.

[19] H. Zhu, A. Abbosh, and L. Guo, "Ultra-wideband unequal in-phase power divider using three-line coupled structure," *Electron. Lett.*, vol. 50, no. 15, pp. 1081–1082, Jul. 2014.

[20] X. Wang, J. Wang, G. Zhang, J.-S. Hong, and W. Wu, "Dual-wideband filtering power divider with good isolation and high selectivity," *IEEE Microw. Wireless Compon. Lett.*, vol. 27, no. 12, pp. 1071–1073, Dec. 2017.

[21] X. Zhao, K. Song, Y. Zhu, and Y. Fan, "Wideband four-way filtering power divider with isolation performance using three parallel-coupled lines," *IEEE Microw. Wireless Compon. Lett.*, vol. 27, no. 9, pp. 800–802, Sep. 2017.

[22] J.-T. Kuo and E. Shih, "Wideband bandpass filter design with three-line microstrip structures," in *IEEE MTT-S Int. Microw. Symp. Dig.*, May 2001, pp. 1593–1596.

[23] S. Sun and L. Zhu, "Capacitive-ended interdigital coupled lines for UWB bandpass filters with improved out-of-band performances," *IEEE Microw. Wireless Compon. Lett.*, vol. 16, no. 8, pp. 440–442, Aug. 2006.

[24] C.-P. Chen, N. Kato, and T. Anada, "Synthesis scheme for wideband filters consisting of three-coupled-lines including the cross-coupling between non-adjacent lines," *IET Microw., Antennas Propag.*, vol. 9, no. 14, pp. 1558–1566, Nov. 2015.

[25] S. Yamamoto, T. Azakami, and K. Itakura, "Coupled strip transmission line with three center conductors," *IEEE Trans. Microw. Theory Techn.*, vol. MTT-14, no. 10, pp. 446–461, Oct. 1966.

[26] D. Pavlidis and H. L. Hartnagel, "The design and performance of three-line microstrip couplers," *IEEE Trans. Microw. Theory Techn.*, vol. MTT-24, no. 10, pp. 631–640, Oct. 1976.

[27] V. K. Tripathi, "On the analysis of symmetrical three-line microstrip circuits," *IEEE Trans. Microw. Theory Techn.*, vol. MTT-25, no. 9, pp. 726–729, Sep. 1977.

[28] J.-Y. Li, C.-H. Chi, and C.-Y. Chang, "Synthesis and design of generalized Chebyshev wideband hybrid ring based bandpass filters with a controllable transmission zero pair," *IEEE Trans. Microw. Theory Techn.*, vol. 58, no. 12, pp. 3720–3731, Dec. 2010.

[29] R. Zhang and L. Zhu, "Synthesis and design of wideband dual-band bandpass filters with controllable in-band ripple factor and dual-band isolation," *IEEE Trans. Microw. Theory Techn.*, vol. 61, no. 5, pp. 1820–1828, May 2013.

[30] R. Zhang and L. Zhu, "Synthesis of dual-wideband bandpass filters with source-load coupling network," *IEEE Trans. Microw. Theory Techn.*, vol. 62, no. 3, pp. 441–449, Mar. 2014.

[31] R. J. Cameron, "General coupling matrix synthesis methods for Chebyshev filtering functions," *IEEE Trans. Microw. Theory Techn.*, vol. 47, no. 4, pp. 433–442, Apr. 1999.

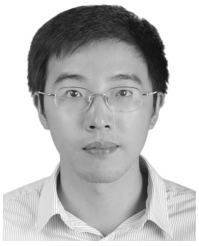

XI YU (S'13) received the B.Eng. degree in electronic engineering from the University of Electronic Science and Technology of China, Chengdu, China, in 2013, where he is currently pursuing the Ph.D. degree. His research interests include the synthesis and design of microwave filters and antennas, multi-functional integrated devices, and the wireless power transfer system.

SHENG SUN (S'02–M'07–SM'12) received the B.Eng. degree in information engineering from Xi'an Jiaotong University, Xi'an, China, in 2001, and the Ph.D. degree in electrical and electronic engineering from Nanyang Technological University (NTU), Singapore, in 2006.

From 2005 to 2006, he was with the Institute of Microelectronics, Singapore. From 2006 to 2008, he was a Post-Doctoral Research Fellow with NTU. He was a Humboldt Research Fellow with the Institute of Microwave Techniques, University of Ulm, Ulm, Germany, from 2008 to 2010, and a Research Assistant Professor with The University of Hong Kong, Hong Kong, from 2010 to 2015. Since 2015, he has been a Professor with the University of Electronic Science and Technology of China, Chengdu, China. He has co-authored one book and two book chapters, and over 140 journal and conference publications. His current research interests include electromagnetic theory, computational mathematics, multiphysics, numerical modeling of planar circuits and antennas, microwave passive and active devices, and the microwave- and millimeter-wave communication systems.

Dr. Sun is currently a member of the Editor Board of the *International Journal of RF and Microwave Computer Aided Engineering* and the *Journal of Communications and Information Networks*. He was a recipient of the ISAP Young Scientist Travel Grant, Japan, in 2004. He was a co-recipient of the several best paper awards at international conferences. He received the Outstanding Reviewer Award from the IEEE MICROWAVE AND WIRELESS COMPONENTS LETTERS in 2010. He was a recipient of the General Assembly Young Scientists Award from the International Union of Radio Science in 2014 and the Hildegard Maier Research Fellowship of the Alexander Von Humboldt Foundation, Germany, in 2008. He was an Associate Editor of the *IEICE Transactions on Electronics* from 2010 to 2014 and a Guest Associate Editor of the *Applied Computational Electromagnetics Society's Journal* in 2017 and 2018. He is a Guest Editor of the *IEEE Journal on Multiscale and Multiphysics Computational Techniques* in 2018 and an Associate Editor of the IEEE MICROWAVE AND WIRELESS COMPONENTS LETTERS since 2017.